Computers and Electrical Engineering 81 (2020) 106454

Contents lists available at ScienceDirect

Computers and Electrical Engineering

journal homepage: www.elsevier.com/locate/compeleceng

Detection of apple defect using laser-induced light backscattering imaging and convolutional neural network ☆

Ang Wu, Juanhua Zhu*, Taiyong Ren

College of Mechanical and Electrical Engineering, Henan Agricultural University, No. 63 Agricultural Road, Zhengzhou 450002, China

ARTICLE INFO

Article history:
Received 15 May 2019
Revised 24 July 2019
Accepted 2 September 2019
Available online 14 November 2019

Keywords:
Apple defect
Convolutional neural network
Laser backscattering imaging
Image recognition

ABSTRACT

The similarity of gray characteristics and shapes of the defects, stems, and calyxes in apple images is a difficult challenge for automatic identification and detection of apple defects in the machine vision field. This paper attempts towards finding an automatic and efficient way to identify apple defects. An automatic detection method is proposed for apple defects based on laser-induced light backscattering imaging and convolutional neural network (CNN) algorithm. Laser backscattering spectroscopic images of apples are obtained using semiconductor laser. We take preprocessing steps to get the finest image dataset for CNN. An AlexNet model with an 11-layer structure is established and trained to identify apple defects. We analyze how well the model does with the recognition effects of apple defects. The proposed CNN model for the detection of apple defects achieves a higher recognition rate of 92.5%, and the accuracy is better than conventional machine learning algorithms. The method based on laser backscattering imaging analysis and CNN theory provides an idea and theoretical basis for efficient, non-destructive, and online detection of fruits quality.

1. Introduction

Detection and classification of fruits quality are critical to improving the economic value-added of fruits. Traditional manual detection methods are inefficient and can only obtain external quality information of fruit. Numerous researchers have studied the fruit quality detection methods to improve the accuracy and rapidity of diagnosis result, such as machine vision [1], multispectral technology [2], infrared spectroscopy [3], and hyperspectral imaging methods [4]. Machine vision methods are relatively mature for the surface detection of apples, such as shape, size, and color, but they are difficult to detect the internal defects. The methods, such as near-infrared spectroscopy, multispectral technology, and hyperspectral imaging, have high accuracy, but they need long detection time and high cost, which limits the application in the fruit detection field.

Laser backscattering method is an optical technique which can be used for nondestructive detection of fruit samples [5]. Laser beams with high coherence illuminate the surface of the apple, part of which are absorbed by the tissue, and part of which are backscattered to form speckles on the apple fruit surface. This halo information formed on the surface of the

☆ This paper is for CAEE special section SI-aicv3. Reviews processed and recommended for publication to the Editor-in-Chief by Associate Editor Dr. Huimin Lu.

* Corresponding author.
E-mail address: zhujh88@sina.com (J. Zhu).

https://doi.org/10.1016/j.compeleceng.2019.106454
0045-7906/

apple can characterize the chemical compositions and physical properties. The laser backscattering images collected by a camera can be used to detect the fruit quality.

The gray characteristics and shapes of the defects, stems, and calyxes are similar in apple images, and thus it is necessary to study appropriate algorithms to correctly identify the defects.

In the last ten years, researchers have done extensive and meaningful research on convolutional neural network (CNN) to optimize architecture and improve algorithm performance, and many research results on the detection and classification of agricultural product defects based on CNN have also been reported. To achieve a fast and accurate diagnosis of apple defects, it is feasible to apply CNN to automatically analyze and process apple defects.

The motivation of this paper is to realize the automatic diagnosis of apple defects using CNN to classify the acquired laser scattering images. The main contributions of this work are:

1 A laser-induced backscattering imaging system is built to obtain high-quality laser images.
2 The CNN method is applied to detect apple defects. It can correctly and effectively identify the defects, stems, calyxes, and normal regions of apples.
3 For classification purposes, we also use other three algorithms: back propagation (BP) neural networks, support vector machine (SVM), and particle swarm optimization (PSO). Experiment results show that the CNN method has a higher recognition accuracy than the others.

The remainder of the article is organized as follows. Section 2 explains the quality detection methods of agricultural products using laser-induced backscattering imaging and related classification algorithms. Section 3 introduces sample preparation, laser-induced backscattering imaging system, datasets preparation, image preprocessing methods, and the details of CNN algorithm. Section 4 presents the detailed results to confirm the performance of the proposed method. Finally, conclusions are summarized in Section 5.

2. Related work

Scholars have carried out a lot of research work using laser scattering to detect agricultural products. Arefi et al. [6] applied biospeckle imaging to identify mealy apples and achieved the classification accuracies for fresh, mealy and, semi-mealy apples of 81%, 77%, and 70%. Hashim et al. [7] used backscattering imaging to assess the postharvest quality of banana fruit effectively. Some other studies applied laser biospeckle technology to classify seeded and seedless watermelons [8], assess sprouting damage in wheat seeds [9], predict quality attributes and ripeness classification of bananas [10], classify potato tubers [11], and detect the climacteric peak of Golden apples [12].

The stem and calyx regions of apple have lower reflectance than healthy surfaces, and their grayscale features and shape are similar to the defects, which can cause frequent detection errors. It is a difficult problem to distinguish fruit defects from fruit stems and calyxes correctly. Pineda et al. [13] criminated the defect, calyx and stem for apple quality control using hyperspectral imaging, and achieved the defect detection rate of 95%. Mohana et al. [14] extracted the shape features of the detected candidate objects and recognized stem–calyx regions from true defects using SVM classifier. Many methods, such as BP neural networks [15], SVM [16], brain intelligence [17], and deep learning [18], are applied to diagnose defects in crops [19,20] to improve the accuracy and rapidity of the diagnosis results.

CNN has more outstanding performance than traditional machine learning and is widely used in computer vision and pattern recognition. Its advantages are reflected in the following aspects: CNN can automatically learn features from sample datasets; it has a certain degree of invariance to geometric transformation, deformation, and illumination; it can obtain features directly from the convolutional layer of neural network and can be used for higher-level feature recognition than manual design, which can overcome manual limitations and exhibit great reliability. CNN is regarded as one of the best classification methods and has wide application prospect in pattern recognition fields.

So far, no research published explores related CNN for apple defect detection based on laser backscatter imaging. The goal of this study is to construct a CNN model to achieve fast, accurate, and automatic identification of the defects, stems, and calyxes of apple images by laser-induced light backscattering imaging. The main purpose of the research is to provide a new detection idea and method for the detection of apple defects.

3. Materials and methods

3.1. Materials preparation

A total of 500 ‘Aksu Fuji’ apple samples about the same size (equatorial diameter 80–100 mm) purchased from the fruit market are used in this study. 250 normal apple samples with uniform quality are selected for obtaining three groups of laser speckle image data, namely stems, calyxes, and normal equatorial regions. Another 250 apple samples with defects, such as rot, insect injury, and bruise, are selected for obtaining the defect image data. The diameter of the defective regions is 5–20 mm. The apple sample images are shown in Fig. 1.

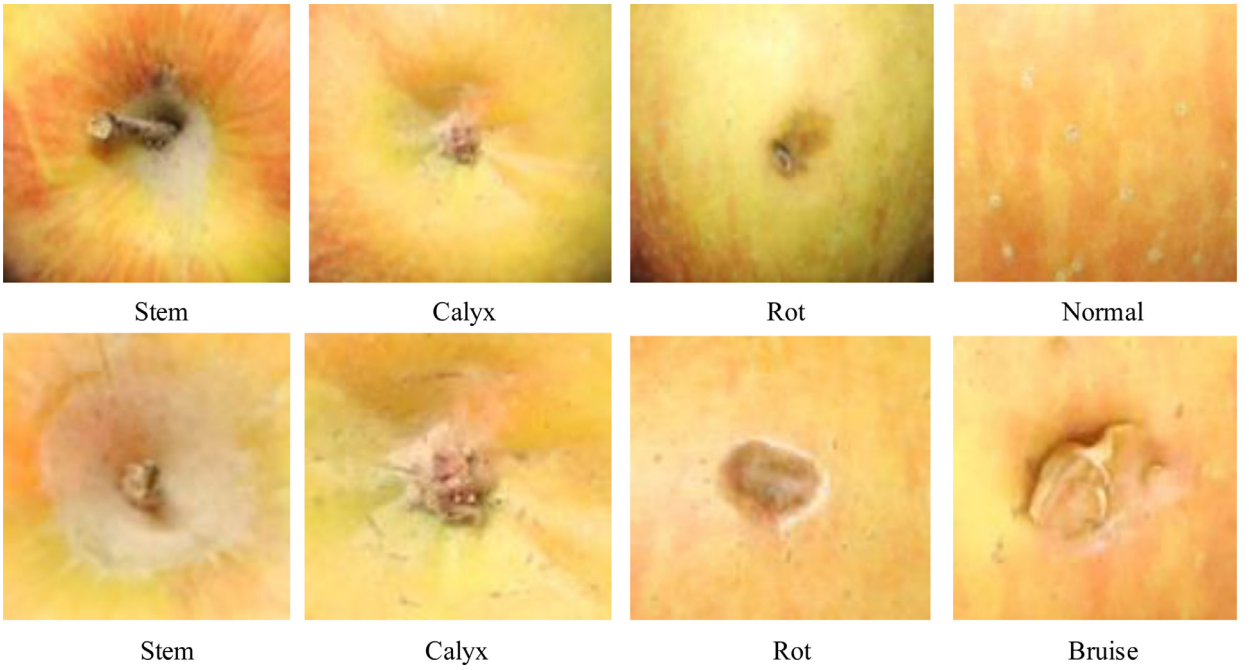

Fig. 1. Apple samples.

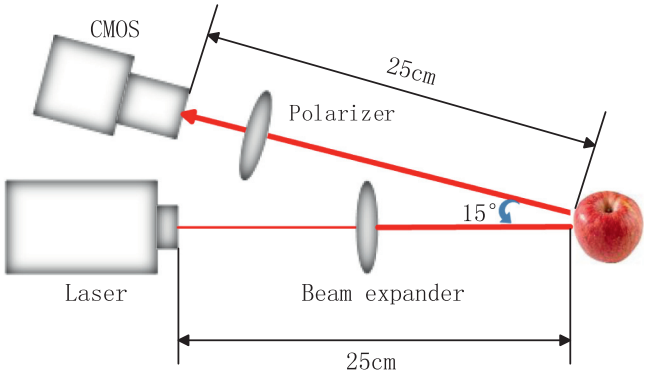

Fig. 2. Experimental setup of laser speckle imaging.

3.2. Laser-induced backscattering imaging system

Apple laser speckle images were obtained using a laser-induced backscattering imaging system, which mainly included a laser, a beam expander with 5 times expansion and 30 mm maximum spot diameter, a complementary metal oxide semiconductor (CMOS) color camera with a zoom lens (focal length of 18–135 mm and f/3.5–5.6), and a polarizer (Fig. 2). The semiconductor laser with 25 mW power, 635 nm wavelength, and 5.2 mm beam size at the aperture is selected as the light source according to the effects of laser speckle imaging at different wavelengths and powers. The laser beams expanded by a beam expander provide uniform light intensity into the apple tissue. The backscattering images (5472 pixels × 3648 pixels) of apple samples are obtained by the CMOS camera. The apple surface is smooth and liable to cause specular reflection when the incident light strikes on it such that the polarizer is placed in front of the camera to eliminate the specular reflection.

Detection system parameters are adjusted to ensure that the acquired image is clear and undistorted. The distance between the camera lens and the apple sample is 25 cm. When the angle between incident beam and camera is approximately perpendicular to the apple surface, a better speckle image can be obtained.

Through the contrast test, the angle between 0° and 20° has almost no effect on the experimental results. Considering the consistency of the experimental results and the convenience of building the experimental system, the angle is set to 15° To minimize the effects of ambient light on laser light scattering imaging, the image acquisition experiments are performed in a dark box. The parameters of imaging experimental setup are kept unchanged during the experiment.

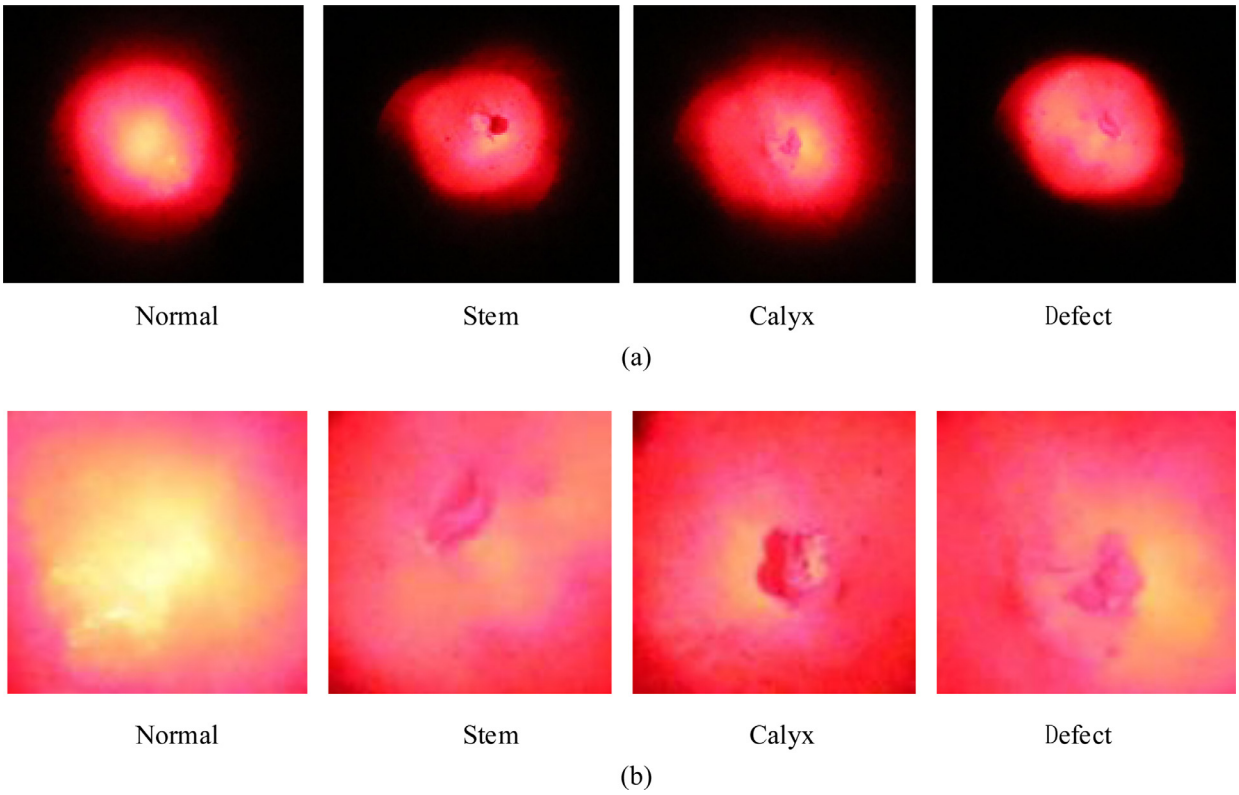

Fig. 3. Laser scattering images of apple samples. (a) original laser scatter images; (b) segmented and normalized laser scattering images.

3.3. Datasets preparation

The defects, such as decay, insect damage, and bruise are classified into the same defect type due to the diversity and complexity of apple defects. Thus the training data and test data are divided into four categories, namely, normal, defect, stem, and calyx. A total of 250 original laser scatter images are selected for each type. The laser backscattering images are shown in Fig. 3(a).

To separate apple defect from stem and calyx accurately, the original images must be preprocessed [21]. The Gaussian filter is used to denoise, and subsequently, the target area, which is the laser irradiation portion, is segmented and extracted. Experiments show that the window of 150*150 pixels not only can contain a full category but also can avoid combining multiple categories into the same window. We extract the 150 × 150 speckle image for subsequent analysis.

The brightness and contrast of the segmented images are normalized. The normalized laser scattering images are shown in Fig. 3(b). Simple cross validation method is used to split sample data into different training set and test set. Firstly, for each category, 200 images are randomly selected as training samples to train the model, and the remaining 50 images are used as test samples to verify the model and parameters. Then, all samples of each category are mixed together, and the training set and the test set are randomly re-selected according to the same ratio of 4 to 1 for the second training and testing. Finally, the loss function is chose to evaluate the optimal model and parameters.

3.4. CNN methods

3.4.1. CNN architecture

CNN based on deep network structure and weight sharing theory can reduce the complexity of the network model and the number of weights, and can avoid the complex feature extraction and data reconstruction process of traditional recognition algorithms using directly the image as the input of the network, such as PSO, SVM, and BP neural network [22,23]. The typical hierarchical structure of CNN has three main neural layers: convolution layer, pooling layer, and fully connected layers. Each transformation layer has a different role, and ultimately, the input data is mapped to the 1D feature vector.

Considering the real-time and accuracy requirements of classification, we design the network architecture of CNN used in our experiments. As observed in Fig. 4, the network contains eleven layers, with an input RGB image size of 150 × 150. Four convolutional layers all use 3 × 3 filters to convolute the whole image, followed by 2 × 2 pooling layers. Full connectivity

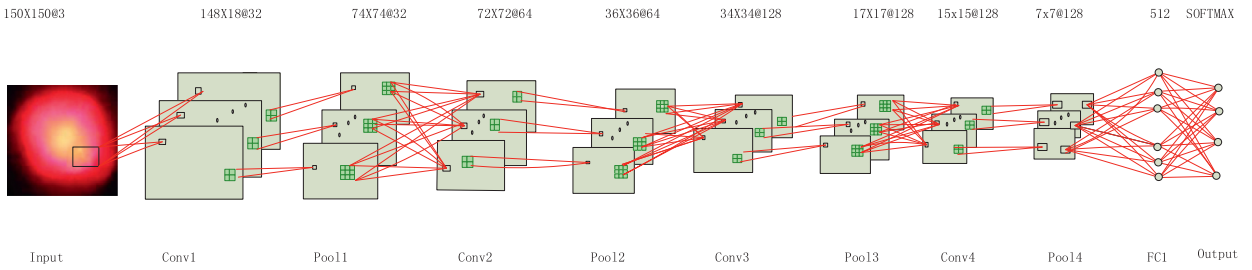

Fig. 4. Network architecture of CNN.

Table 1
Related parameters of CNN.

Layer no.	Type	Kernel size	Moving stride	Neuron size	Maps
1	Input	–	–	150×150	3
2	Conv1	3×3	1	148×148	32
3	Pool1	2×2	2	74×74	32
4	Conv2	3×3	1	72×72	64
5	Pool2	2×2	2	36×36	64
6	Conv3	3×3	1	34×34	128
7	Pool3	2×2	2	17×17	128
8	Conv4	3×3	1	15×15	128
9	Pool4	2×2	2	7×7	128
10	FC1	1×1	1	512×1	1
11	Softmax	Classifier	–	4×1	C

layer fc1 has 512 neurons node. Finally, the output layer obtains the best classification result using Softmax classifier. The relevant parameters are shown in Table 1.

3.4.2. Convolutional layers

The convolutional layers are the core of the whole CNN. They use a variety of kernels to convolute the whole image and perform feature mapping in the intermediate processes to produce various feature map outputs. The designed CNN consists of Conv1, Conv2, Conv3, and Conv4 convolution layers, which are convoluted by 32, 32, 128, and 128 3*3 convolution kernels and input images respectively. Through different convolution operations, the details of the image in different directions can be obtained. The convolution has a certain smoothing effect, which suppresses the noise in the image to some extent. The convolutional layer Conv1 is used to extract different low-level features, such as edges, lines, and corners, from the input image. The other convolutional layers are used to obtain the advanced features. The general formula for convolution operations is obtained as follows:

$$y_j^l = f\left(\sum_{i=1}^{N_j^{l-1}} w_{ij} * x_i^{l-1} + b_j^l\right), j = 1, 2, \cdots \mathrm{M} \tag{1}$$

where y_j^l represents the j-th feature map of the convolutional layer, w_{ij} represents the convolutional kernel, $*$ is the symbol of the convolution operation, x_i^{l-1} is the i-th feature map of the upper layer, b_j^l represents the offset of the j-th convolutional kernel of the current layer, N_j^{l-1} represents the number of feature maps, M is the number of feature maps of the convolution layer and $f(\bullet)$ is the activation function. The often used activation functions include Sigmoid function, Tanh function, and rectified linear unit (ReLU) function in CNN applications. ReLU function is considerably faster to calculate than the others, while still providing good sparse results. Thus, the ReLU function is used as activation function here. The ReLU function is defined by the following:

$$f(x) = \begin{cases} x, & \text{if } x > 0 \\ 0, & \text{otherwise} \end{cases} \tag{2}$$

3.4.3. Pooling layers

The pooling layer is used to reduce the size of the output of the convolutional layer for the purpose of reducing the computational complexity of the subsequent network layers and avoiding overfitting. The most common pooling strategies are average pooling and maximum pooling. The maximum pooling makes the calculation converge quickly and is chosen as the down sampling method in this work. The pooling layers uniformly adopt a 2×2 sub-sampling window. The formula of

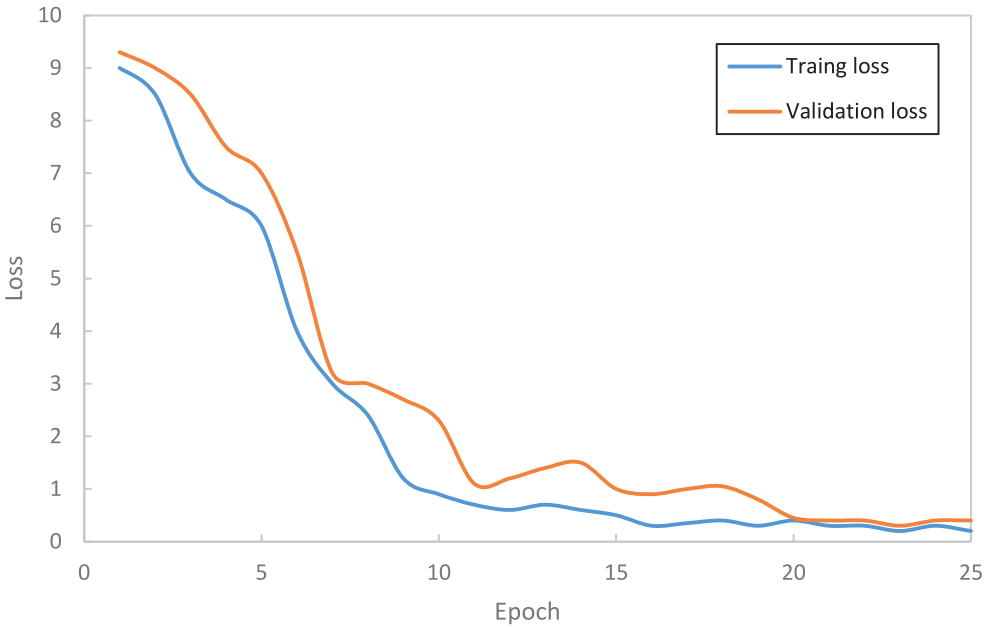

Fig. 5. Curves of cross entropy loss function.

the neuron y on the pooling layer is expressed as shown:

$$y_j^l = f\left(\frac{1}{n}\sum_{i=1}^{N_j^{l-1}} x_i^{l-1} + b_j^l\right) \tag{3}$$

where, y_j^l represents the j-th feature map after pooling, n indicates the window size from the convolutional layer to the sampling layer, $\sum_{i=1}^{N_j^{l-1}} x_i^{l-1}$ means the down sampling process, and $f(\bullet)$ is the pooling function.

The pooling layer is alternately connected to the convolutional layer. With the increase of the network depth, the number of extracted feature maps increases and the size decreases. The features extracted have stronger expressive power.

3.4.4. Fully connected layers

Fully connected layers perform advanced reasoning in neural networks. They are located behind the convolution layers and pooling layers. All inputs of the fully connected layer are connected to all outputs of the front layer. The fully connected layer finally converts the 2D feature map into a 1D feature vector for classification operations [24]. The formula for calculating the connection layer is given by the following:

$$h_{w,b}(x) = f(w^T x + b) \tag{4}$$

where $h_{w,b}(x)$ means the output of neurons, x is the input eigenvector, w represents the weight vector, b represents the offset vector, and $f(\bullet)$ is the activation function.

A certain ratio of neurons is disconnected to reduce the over-fitting and improve the generalization ability of the network using dropout technology when the parameters are updated during training [25]. Here, dropout is used in the fully connected layer and is set to 0.5.

4. Results and discussion

4.1. CNN training process

To test the proposed algorithm, a 2.60 GHz Intel Xeon E5-4607 CPU and 8 GB of memory are used. The detection program is developed in Python 3.7 environment.

From the perspective of training times, the general trend is the more the number of iterations, the higher the recognition accuracy. However, beyond a certain degree, the recognition accuracy of the network model does not continue to increase, and there may be a certain extent of the decline. Therefore, a better recognition accuracy can be obtained by choosing the appropriate number of iterations.

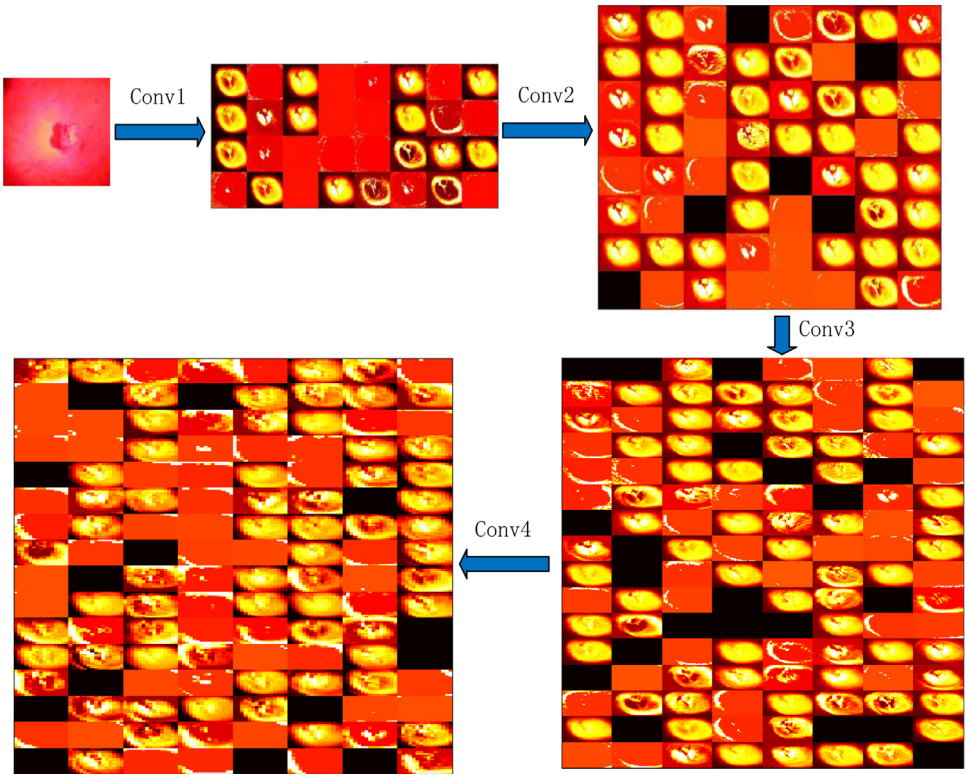

Fig. 6. 2D feature maps from different convolutional layers.

Table 2
Recognition performance using CNN.

recognition result	Normal	Stem	Calyx	Defect
Number of training samples	200	200	200	200
Number of test samples	50	50	50	50
Number of correct recognition	50	45	47	43
Recognition rate (%)	100	90	94	86
Average recognition rate (%)			92.5	

In this work, the cross-entropy error is used as the loss function of training. Fig. 5 shows the Curves of Cross entropy loss function of apple defect classification experiment for each epoch. With the increasing of training iterations, the trend of training and validation loss is decreasing. To achieve higher accuracy without over-fitting the network, the iteration is stopped after 20 epochs. At this point, the test accuracy of the test set is 92.5%.

4.2. Feature visualization analysis

According to the designed CNN network model, the features of the apple laser backscattering images are extracted. Fig. 6 shows the two-dimensional feature maps obtained from different convolutional layers. The characteristics of the model learning are gradually refined from the whole to the local and from the first layer convolution to the fourth layer convolution. The convolved images have the effect of enhancing feature and reducing the noise of the original images. In the pooling layer, the length and width of the image are halved to reduce the amount of data while retaining useful information. It can be observed from the figure that the convolution layer can extract the characteristics of apple well.

4.3. Recognition results analysis

The CNN model is used to identify the defect regions, normal regions, stem regions, and calyx regions of apples. The results are shown in Table 2. The CNN method proposed in this paper has high classification accuracy, and the main reasons are as follows.

1 The normal regions can be fully identified, but the recognition rate of defects is relatively low. The defect and calyx have the highest mutual misjudgment rate. There is also a small amount of misjudgment between the stem and the

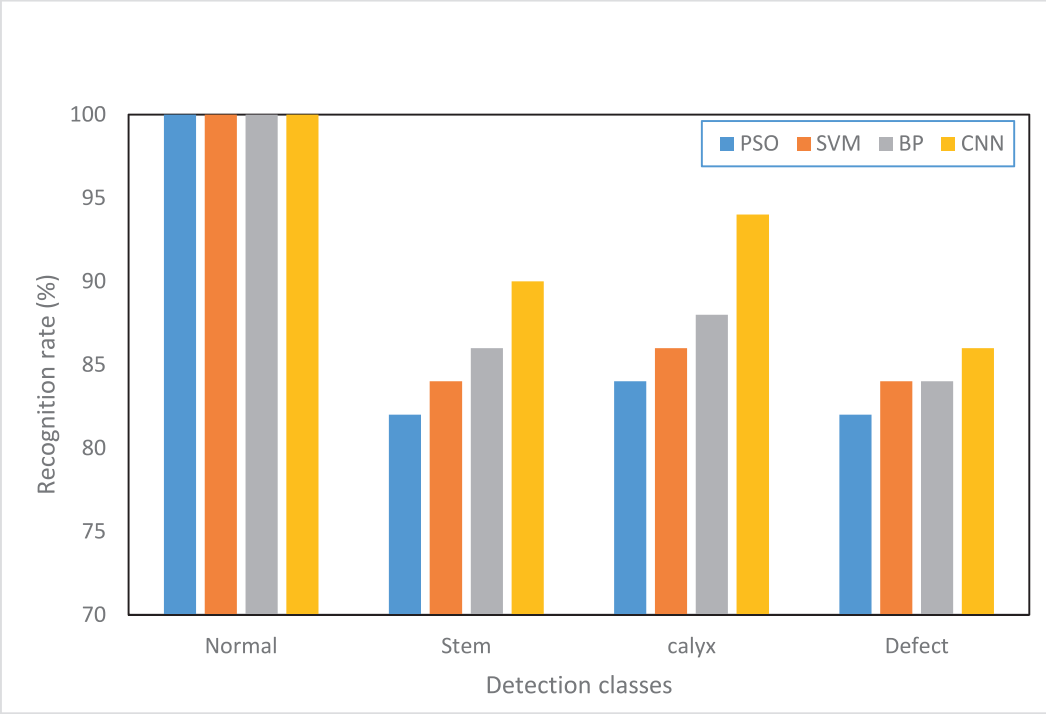

Fig. 7. Comparison results of the proposed CNN with different conventional classification methods.

defect. The misjudgment is mainly due to the similarity of the grayscale features and shapes of some defects, stems, and calyxes. The phenomenon of over-fitting occurs when the CNN layers are further increased due to the limited number of samples. Under the current conditions, the recognition results obtained by using four convolutional layers are relatively good.

2 The nonlinear activation function ReLU increases the non-linear ability of the network in each convolutional layer to better fit the non-linear process. The ReLU function can prevent the gradient from disappearing to a certain extent, and the unilateral inhibition of the function makes the neurons sparsely activated.

3 To compare the recognition rates of mean-pooling and max-pooling, their average recognition rates are 83% and 92.5%, respectively, thus the recognition effect of the max-pooling is better.

4 Dropout is added in the full connection layer to prevent the over-fitting of test samples training. In the process of model training, a certain proportion of hidden layer nodes are set up such that they do not participate in training temporarily.

5 To compare the recognition rates of four common optimizers, namely, Momentum, Adagrad, RMSprop, and Adam, the recognition rates are 86.7%, 87.8%, 90.3%, and 92.5%, respectively. Adam, as a parameter adaptive learning rate method, has the highest recognition rate in this work.

4.4. Comparison between different recognition methods

This paper also compares the CNN algorithm with other algorithms commonly used, such as BP, SVM, and PSO algorithm. Fig. 7 shows the recognition results of the different methods. Among these algorithms, the recognition rate of the proposed approach is the highest.

5. Conclusions and future work

A detection method of apple defects based on laser backscattering imaging and CNN is proposed. The laser backscatter imaging platform is built, and the CNN model of the 11-layer structure is designed. ReLU function and dropout are adopted in training to prevent over-fitting and improve convergence speed. The experimental results show that the method can effectively, non-destructively, and automatically identify the defect regions, normal regions, stem regions, and calyx regions of apples, and the overall recognition rate is over 90%. The method can meet the requirements of the detection of apple defects, especially when the defect regions are similar to the stem and calyx regions in gray characteristics and shapes. The effect of defect recognition based on the CNN model is better than the conventional algorithms. The system has a simple structure and high accuracy, which would probably be used in industrial apple grading, commercially.

Acknowledgements

This research is supported by National Natural Science Foundation of China (No. U1304305); Scientific Research Tackling Key Subject of Henan Province(No. 162102110122, No. 172102210300, No. 182102110116); Key Project of Science and Technology Research of Henan Province Education Department (No. 14B416006, No. 15A416001).

References

[1] Sofu MM, Er O, Kayacan MC, Cetişli B. Design of an automatic apple sorting system using machine vision. Comput Electron Agric 2016;127:395–405.
[2] Peng Y, Lu R. Prediction of apple fruit firmness and soluble solids content using characteristics of multispectral scattering images. J Food Eng 2007;82:142–52.
[3] Qing Z, Ji B, Zude M. Wavelength selection for predicting physicochemical properties of apple fruit based on near-infrared spectroscopy. J Food Qual 2007;30:511–26.
[4] Zhu Q, He C, Lu R, Mendoza F, Cen H. Ripeness evaluation of 'Sun Bright' tomato using optical absorption and scattering properties. Postharvest Biol Technol 2015;103:27–34.
[5] Wu A, Zhu J, Tao Z. Light transmission analysis of laser scattering imaging and Monte Carlo simulation in apple issue. IOP Conf Ser: Mat Sci Eng 2018;392:052026.
[6] Arefi A, Ahmadi Moghaddam P, Hassanpour A, Mollazade K, Modarres Motlagh A. Non-destructive identification of mealy apples using biospeckle imaging. Postharvest Biol Technol 2016;112:266–76.
[7] Hashim N, Adebayo SE, Abdan K, Hanafi M. Comparative study of transform-based image texture analysis for the evaluation of banana quality using an optical backscattering system. Postharvest Biol Technol 2018;135:38–50.
[8] Mohd Ali M, Hashim N, Bejo SK, Shamsudin R. Quality evaluation of watermelon using laser-induced backscattering imaging during storage. Postharvest Biol Technol 2017;123:51–9.
[9] Sutton DB, Punja ZK. Investigating biospeckle laser analysis as a diagnostic method to assess sprouting damage in wheat seeds. Comput Electron Agric 2017;141:238–47.
[10] Adebayo SE, Hashim N, Abdan K, Hanafi M, Mollazade K. Prediction of quality attributes and ripeness classification of bananas using optical properties. Sci Hortic 2016;212:171–82.
[11] Babazadeh S, Ahmadi Moghaddam P, Sabatyan A, Sharifian F. Classification of potato tubers based on solanine toxicant using laser-induced light backscattering imaging. Comput Electron Agric 2016;129:1–8.
[12] Nassif R, Nader CA, Afif C, Pellen F, Le Brun G, Le Jeune B, et al. Detection of golden apples' climacteric peak by laser biospeckle measurements. Appl Opt 2014;53:8276–82.
[13] Pineda I, Alam Md N, Gwun O. Calyx and stem discrimination for apple quality control using hyperspectral imaging. In: Botto-Tobar M, Pizarro G, Zúñiga-Prieto M, D'Armas M, Zúñiga Sánchez M, editors. Technology trends. Cham: Springer International Publishing; 2019. p. 274–87.
[14] Mohana SH, Prabhakar CJ. Extraction of shape features using multifractal dimension for recognition of stem–calyx of an apple. In: Satapathy SC, Biswal BN, Udgata SK, Mandal JK, editors. Proceedings of the 3rd international conference on frontiers of intelligent computing: theory and applications (FICTA) 2014. Springer International Publishing; 2015. p. 357–65.
[15] Zhu J, Wu A, Wang X, Zhang H. Identification of grape diseases using image analysis and BP neural networks. Multimedia Tools Appl 2019.
[16] Wu A, Zhu J, Yang Y, Liu X, Wang X, Wang L, et al. Classification of corn kernels grades using image analysis and support vector machine. Adv Mech Eng 2018;10 1687814018817642.
[17] H. Lu, Y. Li, M. Chen, H. Kim, S. Serikawa. Brain intelligence: go beyond artificial intelligence. eprint arXiv:170601040. (2017) arXiv:1706.01040.
[18] Przybyło J, Jabłoński M. Using deep convolutional neural network for oak acorn viability recognition based on color images of their sections. Comput Electron Agric 2019;156:490–9.
[19] Sabzi S, Abbaspour-Gilandeh Y, García-Mateos G. A new approach for visual identification of orange varieties using neural networks and metaheuristic algorithms. Inf Process Agric 2018;5:162–72.
[20] Chaugule AA, Mali SN. Identification of paddy varieties based on novel seed angle features. Comput Electron Agric 2016;123:415–22.
[21] Serikawa S, Lu H. Underwater image dehazing using joint trilateral filter. Comput Electron Eng 2014;40:41–50.
[22] Park J-K, Kwon B-K, Park J-H, Kang D-J. Machine learning-based imaging system for surface defect inspection. Int J Precis Eng Manuf-Green Technol 2016;3:303–10.
[23] Lu H, Li Y, Uemura T, Kim H, Serikawa S. Low illumination underwater light field images reconstruction using deep convolutional neural networks. Fut Gener Comput Syst 2018;82:142–8.
[24] Voulodimos A, Doulamis N, Doulamis A, Protopapadakis E. Deep learning for computer vision: a brief review. Comput Intell Neurosci 2018;2018:7068349.
[25] Srivastava N, Hinton G, Krizhevsky A, Sutskever I, Salakhutdinov R. Dropout: a simple way to prevent neural networks from overfitting. J Mach Learn Res 2014;15:1929–58.

Ang Wu received the B. Eng. degree from Anhui Engineering University in 2000, and the M. Eng. degree from Hefei University of Technology in 2005. He is currently the lecturer in Henan Agriculture University. He is also working toward the Ph.D. degree from the School of Instrument Science and Opto-Electronics Engineering, Hefei University of Technology. His research interests are machine vision and optical measurement.

Juanhua Zhu received the B. Eng. degree in Communication Engineering from Hefei University of Technology, Hefei, China, in 1999, and the M. Eng. degree in signal and information processing from Hefei University of Technology, Hefei, China, in 2005. She is currently the associate professor in Henan Agriculture University, Zhengzhou, China. Her research interests are video and image processing.

Taiyong Ren received B. Eng. degree in electronic information engineering from Henan Agricultural University, Zhengzhou, China, in 2019. His research focuses on digital image processing and artificial intelligence.